Supplementary Note S1. Verification of FE analysis model

To verify the effectiveness of CVM and FE analysis model of the cushion airbag system, an unmanned aerial vehicle (UAV) and airbag system in reference [22] is selected as the verification model and simulated by CVM. System constitution and design parameters are the same as that in the reference. Assumptions and modeling methods used in this simulation are the same as that in the paper. Figure S1 is a comparison of the deformation configurations during the landing attenuation process between the test results and the simulation results. It can be seen that the simulation results are in agreement with the test results.

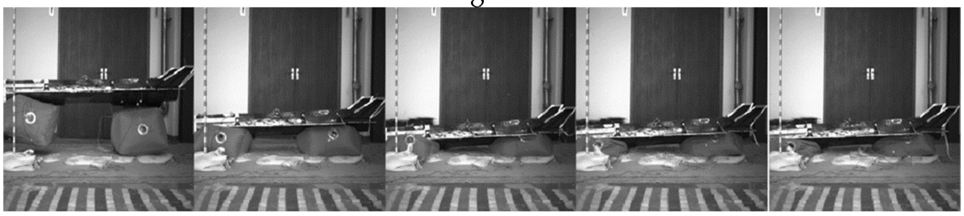

(a) Test results

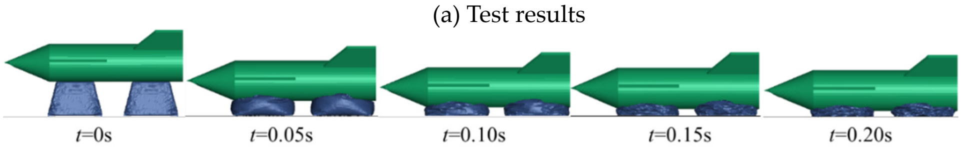

(b) Simulation results

Figure S1. Comparison of deformation configurations

Figure S2 shows the comparison of impact overload from the test results and the simulation results. It can be seen from the figure that the change trends of the test results and simulation results are basically consistent, and the deviations of the maximum overload is within a reasonable range. The reasons for these deviations are that the effect of air resistance is not considered and a simple airbag model * AIRBAG_ WANG_ NEFSKE is used in the analysis model. This work verifies CVM and FE analysis model of the cushion airbag in the landing attenuation process.

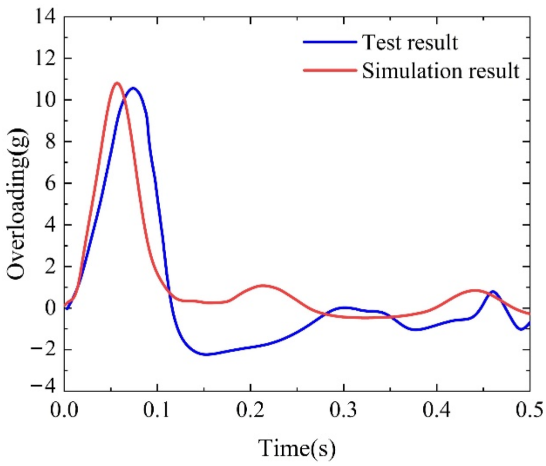

Figure S2. Comparison of dynamic response

Supplementary Note S2. Comparison between the two types of airbags

A model for traditional cylindrical airbags is established with the same section radii and heights as the Model A for origami-inspired airbags, as shown in Figure S3. A finite element model is established and impact dynamic simulations are conducted based on the CVM in software LS-DYNA. The impact overload and the velocity along the Z direction are drawn in Figure S4 (a) and (b).

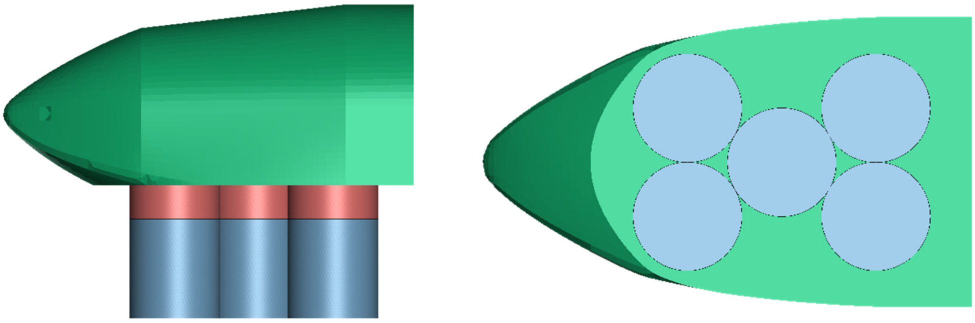

(a) Front-back view (b) Top-down view

Figure S3. Model for traditional cylindrical airbags

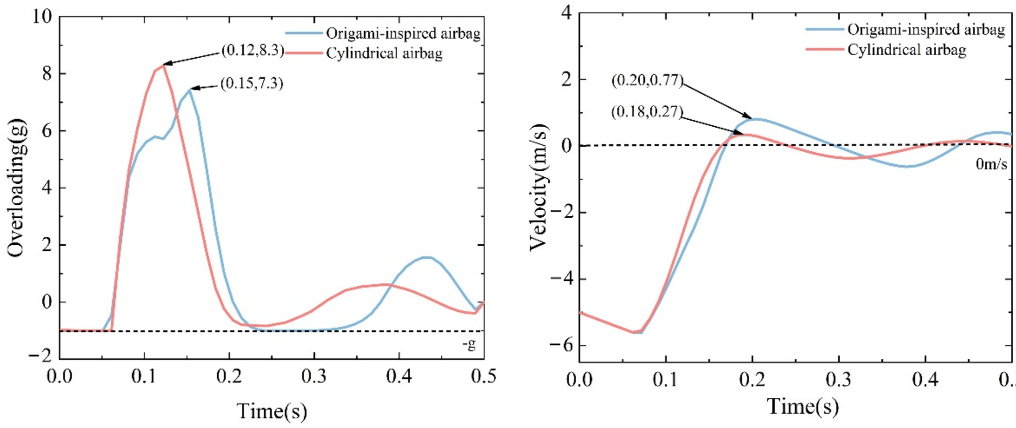

(a) Impact overload (b) Velocity along Z direction

Figure S4. Dynamic response curves of two types of airbags

The results show that the maximum overload experienced by the origami-inspired airbags is 7.3 g, which is lower than the 8.3 g recorded for the cylindrical airbags. It can be seen that origami-inspired airbags can reduce the maximum overload by 12%. From analysis results, it is found that the SEA of origami-inspired airbags is 1648 J/kg while the SEA of cylindrical airbags is 1564 J/kg. The origami-inspired airbags exhibit enhanced specific energy absorption and reduced maximum overload, thereby demonstrating superior cushioning performance.

Supplementary Note S3. Analyses about ground obstacle

The presence of ground obstacles introduces significant challenges to the landing attenuation process, including the risk of large maximum overload, spacecraft rollover, rebound, and bottoming out. These challenges necessitate a detailed study of airbag performance in obstacle-rich environments to ensure the safety. Two types of obstacles on the ground, namely Case S1: a conical obstacle and Case S2: a spherical obstacle, with a radius of 50 mm, are strategically placed directly below the center point of the combined cushion airbag shown in Figure S5. The configurations and stress contours of Case S1 and S2 in the initial state, maximum stress state, and final state are respectively displayed in Figure S6.

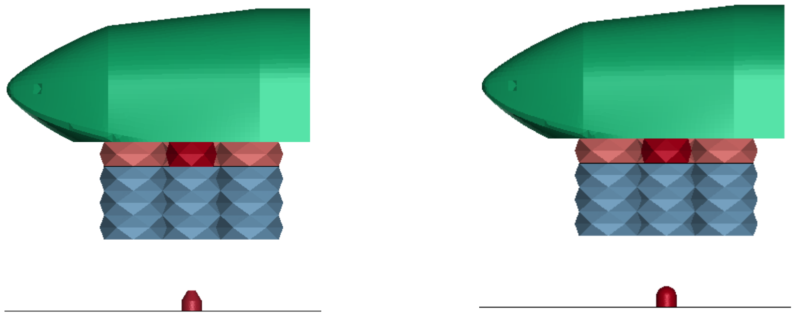

(a) Case S1: conical obstacle (b) Case S2: spherical obstacle

Figure S5. Model B with considering ground obstacles in two cases

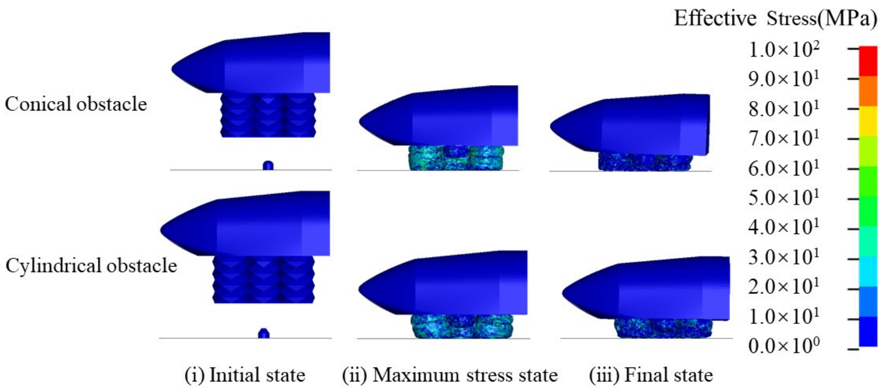

(a) Case S1 (b) Case S2

Figure S6. Stress contours of Model B with considering ground obstacles in two cases

When the airbag is buffered on the ground, the initial stress concentration is observed in the areas of the airbag making contact with the obstacles. This leads to significant local stress and large deformation of the airbag material. In Case S1 and S2 of Figure S4, the maximum local stress values occur at t = 0.11 s and t = 0.12 s as 130 MPa and 127 MPa, respectively. Based on the stress contours of the cushion airbags, the maximum stress strength criterion is utilized to evaluate the strength of the cushion airbags, indicating that the airbag material meets the design strength requirements, showing no failure by puncture even under the stress of impact with obstacles. Importantly, the study observes no rollover phenomenon in the final state of either case. This outcome suggests that the design of the combined cushion airbag system, particularly the anti-rollover supplementary airbags, is highly effective in adapting to ground obstacles.